Bioorganic & Medicinal Chemistry Letters 21 (2011) 4550–4555

Contents lists available at ScienceDirect

Bioorganic & Medicinal Chemistry Letters

journal homepage: www.elsevier.com/locate/bmcl

Discovery of imidazo[1,2-*b*]pyridazines as IKKβ inhibitors. Part 3: Exploration of effective compounds in arthritis models

Hiroki Shimizu [a,*], Tomonori Yamasaki [a], Yoshiyuki Yoneda [a], Fumihito Muro [a], Tomoaki Hamada [a], Takanori Yasukochi [b], Shinji Tanaka [a], Tadashi Toki [a], Mika Yokoyama [a], Kaoru Morishita [a], Shin Iimura [a]

[a] *R&D Division, Daiichi Sankyo Co., Ltd., 1-16-13 Kitakasai, Edogawa-ku, Tokyo 134-8630, Japan*
[b] *Research Department II, Daiichi Sankyo RD Associe Co., Ltd., 1-2-58 Hiromachi, Shinagawa-ku, Tokyo 140-8710, Japan*

ARTICLE INFO

Article history:
Received 30 March 2011
Revised 27 May 2011
Accepted 31 May 2011
Available online 6 June 2011

Keywords:
Inhibitor
IKK
TNF
Imidazo[1,2-*b*]pyridazine
Collagen-induced arthritis
Pharmacokinetic

ABSTRACT

We have discovered imidazo[1,2-*b*]pyridazine derivatives that show suppressive activity of inflammation in arthritis models. We optimized the substructures of imidazo[1,2-*b*]pyridazine derivatives to combine potent IKKβ inhibitory activity, TNFα inhibitory activity *in vivo* and excellent pharmacokinetics. The compound we have acquired, which had both potent activities and good pharmacokinetic profiles based on improved physicochemical properties, demonstrated efficacy on collagen-induced arthritis models in mice and rats.

Nuclear factor-κB (NF-κB) is a transcription factor that has a crucial part in the immune system.[1,2] NF-κB plays a number of important roles such as immune response, inflammation, cell proliferation, survival and cell death by regulating the expression of a variety of genes of proteins including pro-inflammatory cytokines (e.g., TNFα, IL-1, IL-6), chemokines, anti-apoptotic proteins, adhesion molecules, osteoclastogenesis-related factors and inducible proteins.[3–7] NF-κB is implicated in the pathogenesis of multiple inflammatory diseases and autoimmune diseases including rheumatoid arthritis. It is observed that NF-κB is highly active in the site of inflammation.[3–5,8]

There are some signal transduction cascades for the activation of NF-κB.[6d,9] In the classical (canonical) pathway, known as one of the major pathways, IKK complex (IKKα/IKKβ/NEMO) plays an important role in activating NF-κB (RelA/p50).[9,10] RelA/p50 exists as an inactive complex associated with IκB. The phosphorylation of IκB by the IKK complex and subsequent K48-linked polyubiquitination lead to the degradation of IκB. The released RelA/p50 promotes transcription of genes of pro-inflammatory cytokines and other inducible proteins in nucleus.

Of the IKK components, IKKβ is essential in the phosphorylation of IκB. It is anticipated that a potent IKKβ inhibitor could be a promising anti-inflammatory agent.[2a,11,12] A number of pharmaceutical companies and research institutes have tried to develop IKKβ inhibitors.[13] We also continued our effort to acquire orally active small molecule IKKβ inhibitors.[14,15] We have confirmed the potency of imidazo[1,2-*b*]pyridazine derivatives as IKKβ inhibitors as we have reported compounds **1** and **2** showed potent IKKβ inhibitory activity (Fig. 1).[14] Furthermore, compounds **3** and **4** exhibited strong

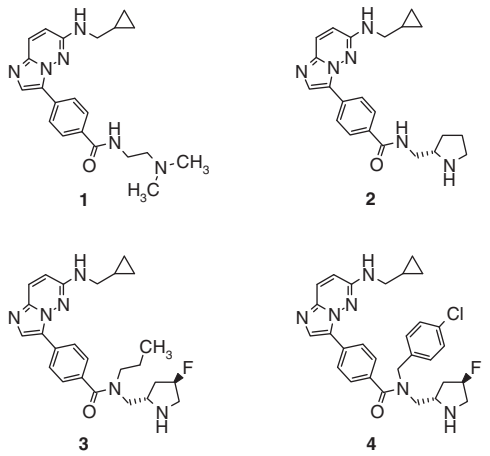

Figure 1. Potent IKKβ inhibitors with an imidazo[1,2-*b*]pyridazine scaffold.[14,15]

* Corresponding author. Tel.: +81 3 3680 0151; fax: +81 3 5696 8609.
E-mail address: shimizu.hiroki.hu@daiichisankyo.co.jp (H. Shimizu).

0960-894X/$ - see front matter © 2011 Elsevier Ltd. All rights reserved.
doi:10.1016/j.bmcl.2011.05.115

TNFα inhibitory activity in mice.[15] In the following step, it becomes important to find compounds that show efficacy in arthritis models to develop an anti-inflammatory agent.

To resolve the issue, we need to explore the compounds which combine potent IKKβ inhibitory activity, TNFα inhibitory activity in vivo and good pharmacokinetic properties. We consider that compounds **3** and **4**, which exhibited TNFα inhibitory activity in vivo, did not necessarily show satisfactory plasma concentration for continuously administrated studies.[15] As a result, we decided to further explore and modify compounds **1** and **2** with the goal to increase plasma concentrations and functional activity to help improve efficacy in arthritis models.

To begin with, we planned to modify the benzamide moiety in the 3-position of imidazo[1,2-*b*]pyridazine. It was assumed that the benzamide moiety affects the pharmacokinetic properties.[16] The results are summarized in Table 1. Compounds **5d** and **5e**, which have 2-fluorobenzamide moiety, showed greater TNFα inhibitory activity in vivo. Improvement was considered to be caused by the enhancement of oral absorption, which was indicated as the improvement of values in the permeability test with Madin–Darby canine kidney (MDCK) cells (P_{app}: **5d** = 6.2, **5e** = 5.6 compared with **1** = 2.1, **5a** = 2.3 ($\times 10^{-6}$ cm/s)).[17] The improvement of permeability is possibly due to the enhancement of hydrophobicity as seen in the distribution coefficient values, the masking effect of amide NH moiety by the formation of weak internal hydrogen bonding between fluorine and NH of benzamide and/or the weakening of crystalinity.[16,18] However, there was concern that the clearance of **5d** and **5e** seemed to be higher as observed in the decrease of plasma concentration of **5d** and **5e** compared with **1** and **5a** at 90 min after oral administration. To reduce the clearance, we tried to change the terminal amine substructures such as pyrrolidin-2-ylmethyl derivatives **5f** and **5g**.[15] We found that **5g** showed potent IKKβ inhibitory activity, TNFα inhibitory activity and a higher level of plasma concentration (MDCK P_{app}: **5g** = 4.2×10^{-6} cm/s). The 2- or 3-methyl benzamide group such as **5b** or **5c** led to the decrease in IKKβ inhibitory activities. IKKβ inhibitory activity of **5b** decreased 10-fold than that of **5c**. It is considered that the methyl group interfered with the planarity of phenyl moiety and the imidazo[1,2-*b*]pyridazine scaffold. In the same reason, 3-pyridyl derivative **5j** was more potent than 2-pyridyl derivative **5k** in cell-free inhibitory assay. Compounds **5i** and **5j** showed lower inhibitory activities in mouse whole blood cell assay for IKKβ inhibitory activities because of lower permeability as shown in the PAMPA values in Table 1. The substitution of benzamide to five-membered heteroaryl carbamoyl moieties such as **5l** and **5m** reduced IKKβ inhibitory activities. It is considered that the difference of angle from 1,4-phenyl, which is larger in the 2,5-furyl moiety than in the 2,5-thienyl moiety, causes IKKβ

Table 1
The modification of the 3-position of imidazo[1,2-*b*]pyridazine.

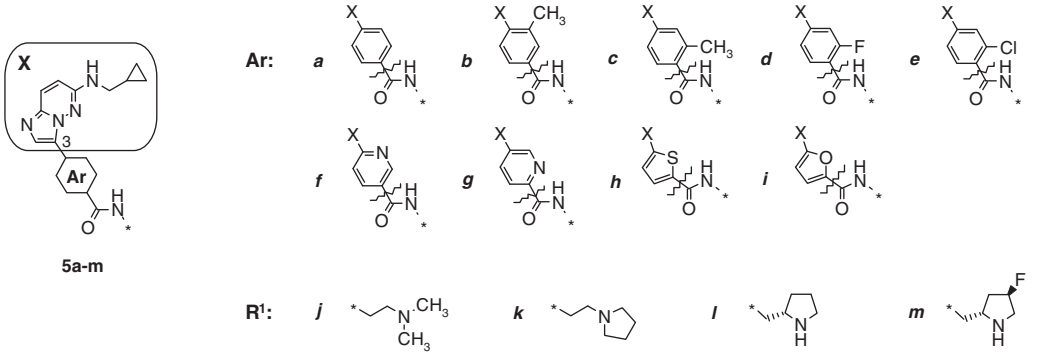

Compds	Ar	R^1	IKKβ[a] IC_{50} (μM)	TNFα production[b] IC_{50} (μM)	Inhibition of TNFα (%) in mice[c]	Plasma level[d] at 30 mg/kg p.o. (μg/ml)	Microsomal stability[e] (%) mice/rats	Log *D*[f] (pH 7.4)	PAMPA[g] P_e ($\times 10^{-6}$ cm/s) (pH 7.4)
1	*a*	*j*	0.20	0.80	10	0.39	71/–[h]	2.5	>50
2	*a*	*l*	0.055	6.8	No inhibition	0.0075	77/–	1.8	0.84
3[i]			0.016	0.17	52	0.16	33/–	3.4	>50
4[i]			0.017	1.2	61	0.45	28/–	5.0	39
5a	*a*	*k*	0.071	0.64	2.0	0.44	75/–	2.6	>50
5b	*b*	*j*	20	–	–	–	–/–	–	–
5c	*c*	*j*	1.9	–	–	–	–/–	–	–
5d	*d*	*j*	0.30	1.2	60	0.11	79/-	2.7	>50
5e	*d*	*k*	0.14	1.0	61	0.29	57/-	2.8	>50
5f	*d*	*l*	0.064	1.3	No inhibition	0.14	85/-	1.8	19
5g	*d*	*m*	0.027	0.26	37	0.38	87/46	3.1	>50
5h	*e*	*l*	0.41	4.1	–	–	92/-	2.2	14
5i	*f*	*j*	0.20	4.0	–	–	100/-	2.0	14
5j	*f*	*k*	0.14	3.7	–	–	100/-	2.0	11
5k	*g*	*k*	0.68	–	–	–	–/–	–	–
5l	*h*	*j*	2.0	–	–	–	–/–	–	–
5m	*i*	*j*	19	–	–	–	–/–	–	–

[a] The method is described in Ref. 14.
[b] Mouse whole blood cell. This method is described in Ref. 15.
[c] The inhibition ratio of TNFα at the oral dose of 30 mg/kg in mice. This method is described in Ref. 15.
[d] Plasma concentration of test compounds at 90 min after oral administration. This method is described in Ref. 15.
[e] The method is described in Ref. 19.
[f] The method is described in Ref. 20.
[g] Parallel artificial membrane permeability assay. This method is described in Ref. 21.
[h] Not tested.
[i] Structure, see Figure 1.

Table 2
The optimization of the 6-position of imidazo[1,2-*b*]pyridazine.

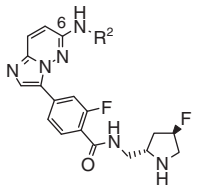

Compds	R^2	IKKβ[a] IC_{50} (μM)	TNFα production[b] IC_{50} (μM)	Inhibition of TNFα (%) in mice[c]	Plasma level[d] at 30 mg/kg p.o. (μg/ml)	Microsomal stability[e] (%) mice/rats	Log *D*[f] (pH 7.4)	PAMPA[g] P_e ($\times 10^{-6}$ cm/s) (pH 7.4)
6a	*n*-Propyl	0.064	0.61	26	0.54	69/–[h]	3.1	>50
6b	*n*-Butyl	0.019	0.47	45	0.60	56/–	3.5	>50
6c	*n*-Pentyl	0.026	0.71	No inhibition	0.093	21/–	4.0	>50
6d	Cyclobutyl	0.017	0.23	56	1.4	54/42	3.3	>50
6e	Cyclopentyl	0.016	0.31	14	0.66	65/–	3.6	>50
6f	$-(CH_2)_2SCH_3$	0.097	1.6	–	–	44/–	2.8	>50
6g	$-(CH_2)_3SCH_3$	0.061	1.2	No inhibition	0.15	13/–	3.0	40
6h	$-(CH_2)_3F$	0.12	1.5	32	0.48	85/47	2.5	33
6i	$-(CH_2)_4F$	0.043	1.2	57	0.42	80/18	2.8	>50
6j	$-(CH_2)_5F$	0.029	0.71	18	0.11	44/–	3.3	37

[a-h]See notes of Table 1.

inhibitory activities to decrease more in **5m**. The 2-chlorobenzamide **5h,** instead of 2-fluorobenzamide **5f,** was not adequate.

To further optimize **5g**, we explored the substituent located at the 6-position of imidazo[1,2-*b*]pyridazine. The results are summarized in Table 2. The compounds with cycloalkyl moieties such as **6d** and **6e** were more potent than *n*-alkyl (**6a–6c**) or substituted alkyl moieties (**6f–6j**) in IKKβ inhibitory activity and/or TNFα inhibitory activity in mouse whole blood cell assay. The plasma concentrations were moderate in most compounds, and we could see the tendency for plasma levels to become lower as the sizes of 6-substituents become larger. The same tendency can be seen in microsomal stability values.

We discovered that compound **6d** possesses an excellent profile with potent in vitro and in vivo inhibitory activities and higher plasma concentrations based on good physicochemical properties (MDCK P_{app}: **6d** = 7.0×10^{-6} cm/s).[22] Pharmacokinetic properties of **5g** and **6d** in mice and rats are displayed in Table 3. The pharmacokinetic parameters of **6d** showed remarkable improvement compared with that of **5g** in AUC, C_{max} and clearance. It is considered that the improvement of permeability by the covering of the polar secondary amine in the 6-position of imidazo[1,2-*b*]pyridazine by the more bulky cyclobutyl group would increase the plasma level. The difference can be seen between the species. The difference of the plasma protein binding ratio between mice and rats could be considered as one of the reasons for the difference in species. On the basis of these results, we selected **6d** for further evaluation in rodent arthritis models.

We evaluated **6d** for the anti-inflammatory effect in a collagen-induced arthritis model in mice. Compound **6d** showed efficacy by the reduction of paw swelling at the oral dose of 100 mg/kg.[26] The clinical scores were reduced by 67% (100 mg/kg of **6d** = 2.6 ± 2.3, vehicle control = 8.0 ± 3.2, mean ± SD) when the compound was orally administrated once a day for 14 days after the second challenge of collagen.

Due to the more favorable pharmacokinetic and protein binding properties of **6d** we decided conducted a collagen-induced arthritis model in rats. Compound **6d** significantly reduced paw swelling in a dose-dependent manner (Fig. 2).[27] The paw volume decreased 58% at the 24th day after the first immunization when the compound was orally administrated at the dose of 100 mg/kg once a day for 18 days after the second challenge of collagen. It was observed that **6d** delayed onset, relieved symptoms of paw swelling and suppressed bone destruction. Even though **6d** possesses lower functional activity in the rat whole blood cell assay (mouse: IC_{50} = 0.23 μM vs rat: IC_{50} = 1.7 μM)[28] the superior pharmacokinetic and physical properties led to efficacy.

The conversion of the benzamide moiety and the combination with terminal amine units in the 3-position of imidazo[1,2-*b*]pyridazine was conducted as shown in Schemes 1 and 2. We prepared the benzamide parts as arylboronic acid (pinacol ester) or aryltin derivatives **8a–8i**, which are commercially available or are prepared by the known procedures as indicated in a previous reports.[29] Palladium catalyzed coupling reactions with bromide **7**,[15] followed by hydrolysis of esters as appropriate gave carboxylic acid 10a–10i (Scheme 1). The condensation reaction of **10a–10i** with amine units R^1NH_2 and subsequent deprotection when needed lead to compounds **5a–5m** (Scheme 2).

Synthesis of analogs containing 2-fluoro-*N*-{[(2*S*,4*R*)-4-fluoropyrrolidin-2-yl]methyl}benzamide group (**6a–6j**) at the 3-position of imidazo[1,2-*b*]pyridazine is described in Schemes 3 and 4. The carboxylic acids **14a–14j** were prepared from **12**[14] by way of nucleophilic substitution, conversion and/or protection of the functional

Table 3
Pharmacokinetic properties of **5g** and **6d** in mice and rats at the oral dose of 30 mg/kg.

	Compd	$AUC_{0-24\ h}$ (μg h/ml)	MRT (h)	CL/*F* (ml/min/kg)	V_{dss}/F (L/kg)	$T_{1/2}$(h)	C_{max} (μg/ml)	T_{max} (h)	Protein binding[a]
Mouse[b]	**5g**	0.888	2.3	563	78	0.89	0.26	1.0	90
	6d	1.86	2.0	269	32	0.90	0.75	1.0	94
Rat[c]	**5g**	23.1	4.9	22.2	6.5	2.8	4.1	4.0	98
	6d	95.3	5.1	5.46	1.7	2.4	16	2.8	99

[a] The methods are described in Ref. 23.
[b] Male BALB/c mouse, 30 mg/kg, p.o. This method is described in Ref. 24.
[c] Female Wistar–Lewis rat, 30 mg/kg, p.o. This method is described in Ref. 25.

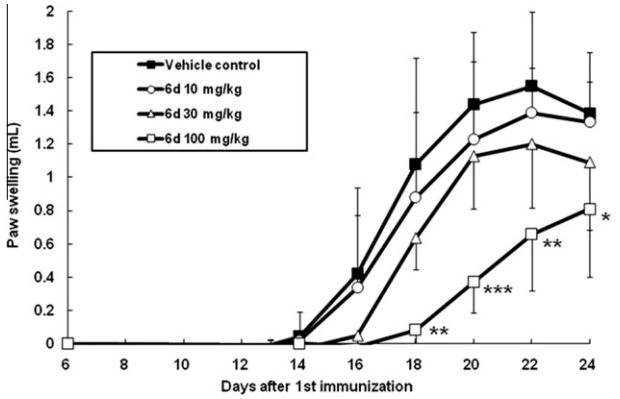

Figure 2. Effect of compound **6d** on the collagen-induced arthritis model in rats. Seven days after the first immunization, the second immunization was performed and each dose of compound **6d** was orally administrated once a day. Data are expressed as mean ± SD. Statistical significance was determined using Dunnett's test. $^{*}p$ <0.05, $^{**}p$ <0.01, $^{***}p$ <0.001 compared with the vehicle control group.

groups and Suzuki–Miyaura coupling reaction (Scheme 3). Compounds **6a–6j** were synthesized by the condensation of **14a–14j** with *tert*-butyl (2*S*,4*R*) 2-(aminomethyl)-4-fluoropyrrolidinecarboxylate, followed by the cleavage of protective groups (Scheme 4).

In conclusion, we successfully optimized the substructures at the 3- and 6-positions of imidazo[1,2-*b*]pyridazine derivatives to combine potent IKKβ inhibitory activity, TNFα inhibitory activity, good pharmacokinetics. During the optimization process it became clear that the 2-fluorobenzamide improved permeability of the compounds while the (2*S*,4*R*)-4-fluoropyrrolidin-2-ylmethyl group improved potency and improved physicochemical properties as demonstrated by compound **5g**. Subsequent modifications of compound **5g** led to the development of **6d** by replacing the

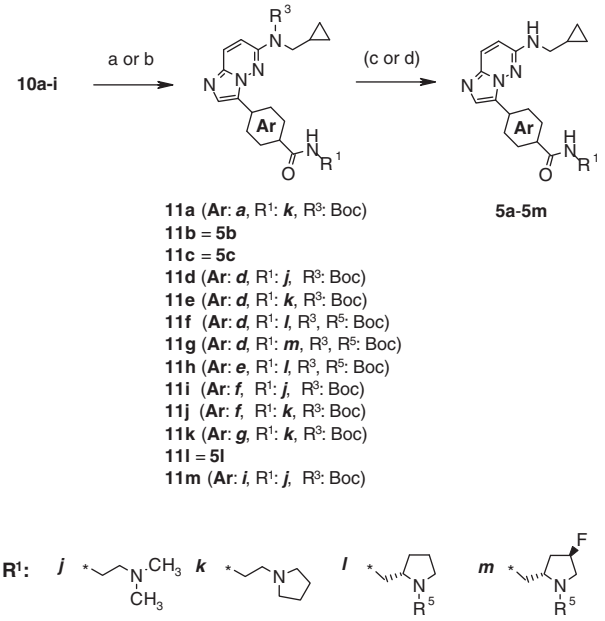

11a (**Ar**: ***a***, R¹: ***k***, R³: Boc)
11b = **5b**
11c = **5c**
11d (**Ar**: ***d***, R¹: ***j***, R³: Boc)
11e (**Ar**: ***d***, R¹: ***k***, R³: Boc)
11f (**Ar**: ***d***, R¹: ***l***, R³, R⁵: Boc)
11g (**Ar**: ***d***, R¹: ***m***, R³, R⁵: Boc)
11h (**Ar**: ***e***, R¹: ***l***, R³, R⁵: Boc)
11i (**Ar**: ***f***, R¹: ***j***, R³: Boc)
11j (**Ar**: ***f***, R¹: ***k***, R³: Boc)
11k (**Ar**: ***g***, R¹: ***k***, R³: Boc)
11l = **5l**
11m (**Ar**: ***i***, R¹: ***j***, R³: Boc)

Scheme 2. Condensation reaction with terminal amine units. Reagents and conditions: (a) R^1NH_2, EDC·HCl, HOBt, Et_3N, CH_2Cl_2, 90% for **11a**, 81% for **11d**, 83% for **11e**, 88% for **11f**, 95% for **11g**, quant. for **11h**, for **11i–11k**, 69% for **11m**; (b) R^1NH_2, DMT-MM, DMF, 94% for **5b**, 94% for **5c**, 57% for **5l**; (c) TFA, CH_2Cl_2, 73% for **5f**, 87% for **5g**, 67% 2 steps for **5i**, 68% 2 steps for **5j**, 59% 2 steps for **5k**, 69% for **5m**; (d) 4 N HCl in 1,4-dioxane, 86% for **5a**, 79% for **5d**, 59% for **5e**, 19% for **5h**.

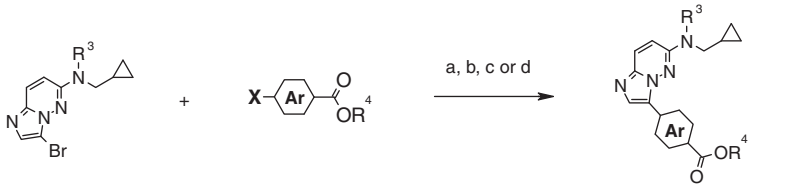

7 (R³: H or Boc)

8a (**Ar**: ***a***, **X**: ***n***, R⁴: Me)
8b (**Ar**: ***b***, **X**: ***o***, R⁴: Me)
8c (**Ar**: ***c***, **X**: ***o***, R⁴: Me)
8d (**Ar**: ***d***, **X**: ***n***, R⁴: H)
8e (**Ar**: ***e***, **X**: ***o***, R⁴: Me)
8f (**Ar**: ***f***, **X**: Br, R⁴: Me)
8g (**Ar**: ***g***, **X**: ***o***, R⁴: Me)
8h (**Ar**: ***h***, **X**: ***n***, R⁴: H)
8i (**Ar**: ***i***, **X**: ***o***, R⁴: Me)

9a (**Ar**: ***a***, R³: Boc, R⁴: Me)
9b (**Ar**: ***b***, R³: H, R⁴: Me)
9c (**Ar**: ***c***, R³: H, R⁴: Me)
9d = **10d**
9e (**Ar**: ***e***, R³: Boc, R⁴: Me)
9f (**Ar**: ***f***, R³: Boc, R⁴: Me)
9g (**Ar**: ***g***, R³: Boc, R⁴: Me)
9h = **10h**
9i (**Ar**: ***i***, R³: Boc, R⁴: Me)

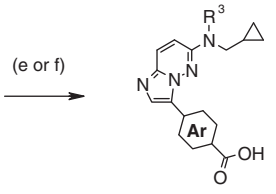

10a (**Ar**: ***a***, R³: Boc)
10b (**Ar**: ***b***, R³: H)
10c (**Ar**: ***c***, R³: H)
10d (**Ar**: ***d***, R³: Boc)
10e (**Ar**: ***e***, R³: Boc)
10f (**Ar**: ***f***, R³: Boc)
10g (**Ar**: ***g***, R³: Boc)
10h (**Ar**: ***h***, R³: H)
10i (**Ar**: ***i***, R³: Boc)

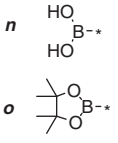

Scheme 1. Preparation of arylcarboxylic acid derivatives. Reagents and conditions: (a) **8**, $PdCl_2(dppf)\cdot CH_2Cl_2$, $K_3PO_4\cdot nH_2O$, 1,4-dioxane–H_2O (9:1), 80–95 °C, 93% for **9a**, 75% for **9b**, 46% for **9c**, quant. for **9e**, 62% for **9g**, 97% for **9i**; (b) **8d**, $PdCl_2(PPh_3)_2$, 2 M K_2CO_3 aq., 1,4-dioxane, 90 °C, 81% for **10d**; (c) **8f**, hexamethylditin, $Pd_2(dba)_3$, P(*t*-Bu)$_3$, 1,4-dioxane, 90 °C, 18% for **9f**; (d) **8h**, $Pd(PPh_3)_4$, Cs_2CO_3, DMF–EtOH–H_2O (7:2:3), microwave irradiation 130 °C, 5 min, 66% for **10h**; (e) 1 N NaOH aq., MeOH, 82% for **10b**, 82% for **10c**, 51% for **10f**, 88% for **10g**, 90% for **10i**; (f) 1 N NaOH aq, THF–MeOH (4:1), 97% for **10a**, 66% for **10e**. Boc: *tert*-butoxycarbonyl.

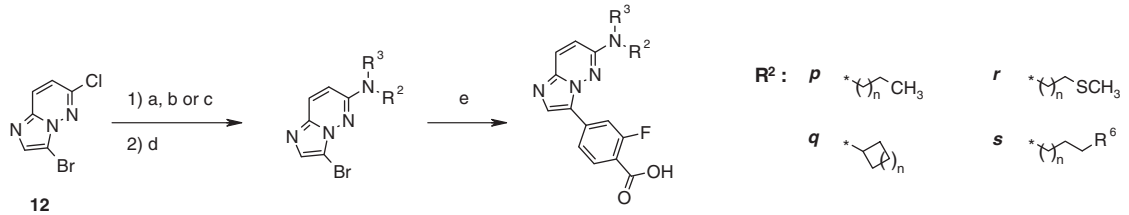

13a (R^2: ***p***, n = 1)
13b (R^2: ***p***, n = 2)
13c (R^2: ***p***, n = 3)
13d (R^2: ***q***, n = 1)
13e (R^2: ***q***, n = 2)
13f (R^2: ***r***, n = 1)
13g (R^2: ***r***, n = 2)
13h (R^2: ***s***, n = 1)
13i (R^2: ***s***, n = 2)
13j (R^2: ***s***, n = 3)

14a (R^2: ***p***, R^3: Boc, n = 1)
14b (R^2: ***p***, R^3: Boc, n = 2)
14c (R^2: ***p***, R^3: Boc, n = 3)
14d (R^2: ***q***, R^3: Boc, n = 1)
14e (R^2: ***q***, R^3: H, n = 2)
14f (R^2: ***r***, R^3: Boc, n = 1)
14g (R^2: ***r***, R^3: Boc, n = 2)
14h (R^2: ***s***, R^3: Boc, n = 1)
14i (R^2: ***s***, R^3: Boc, n = 2)
14j (R^2: ***s***, R^3: Boc, n = 3)

Scheme 3. Preparation of 2-fluorobenzoic acid derivatives. Reagents and conditions: (a) R^2NH_2, 120 °C for **13a** (R^3: H), for **13b** (R^3: H), for **13c** (R^3: H), 79% for **13e** (R^3: H); (b) R^2NH_2, Et_3N, NMP, 125–140 °C, 95% for **13d** (R^3: H), 79% for **13f** (R^3: H), 96% for **13g** (R^3: H); (c-1) R^2NH_2, NMP, 125 °C, 99% for **13h** (R^3: H, R^6: OH), 96% for **13i** (R^3: H, R^6: OH), 88% for **13j** (R^3: H, R^6: OH); (c-2) PMBCl, NaH, DMF then CAN, MeOH–H_2O (9:1), 56% for **13h** (R^3: PMB, R^6: OH), 49% for **13i** (R^3: PMB, R^6: OH), 45% for **13j** (R^3: PMB, R^6: OH); (c-3) MsCl, Et_3N, CH_2Cl_2, 0°C, 88% for **13h** (R^3: PMB, R^6: OMs), 82% for **13i** (R^3: PMB, R^6: OMs), 48% for **13j** (R^3: PMB, R^6: OMs); (c-4) TBAF, THF, 60 °C, for **13h** (R^3: PMB, R^6: F), 83% for **13i** (R^3: PMB, R^6: F), 85% for **13j** (R^3: PMB, R^6: F); (c-5) TFA, CH_2Cl_2, 79% 2 steps for **13h** (R^3: H, R^6: F), 94% for **13i** (R^3: H, R^6: F), 97% for **13j** (R^3: H, R^6: F); (d) $(Boc)_2O$, DMAP, CH_2Cl_2, 60 °C, 60% 2 steps for **13a** (R^3: Boc), 88% 2 steps for **13b** (R^3: Boc), 86% 2 steps for **13c** (R^3: Boc), 80% for **13d** (R^3: Boc), No reaction. **13e** (R^3: H) was recovered, 89% 2 steps for **13f** (R^3: Boc), 94% for **13g** (R^3: Boc), 93% for **13h** (R^3: Boc, R^6: F), quant. for **13i** (R^3: Boc, R^6: F), 92% for **13j** (R^3: Boc, R^6: F); (e) 4-Carboxy-3-fluorophenylboronic acid, $PdCl_2(PPh_3)_2$, 2 M K_2CO_3 aq., 1,4-dioxane 90 °C, 55% for **14a**, 79% for **14b**, 94% for **14c**, 82% for **14d**, 51% for **14e**, quant. for **14f**, 88% for **14g**, quant. for **14h**, 97% for **14i**, 97% for **14j**. PMB: *p*-methoxybenzyl, OMs: methanesulfonyloxy.

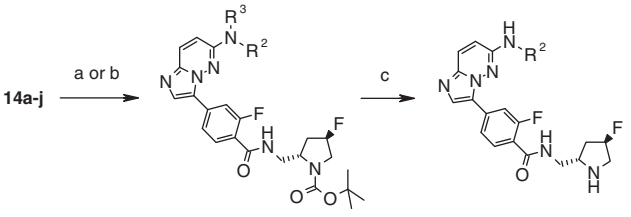

15a (R^2: ***p***, R^3: Boc, n = 1)
15b (R^2: ***p***, R^3: Boc, n = 2)
15c (R^2: ***p***, R^3: Boc, n = 3)
15d (R^2: ***q***, R^3: Boc, n = 1)
15e (R^2: ***q***, R^3: H, n = 2)
15f (R^2: ***r***, R^3: Boc, n = 1)
15g (R^2: ***r***, R^3: Boc, n = 2)
15h (R^2: ***s***, R^3: Boc, R^6: F, n = 1)
15i (R^2: ***s***, R^3: Boc, R^6: F, n = 2)
15j (R^2: ***s***, R^3: Boc, R^6: F, n = 3)

Scheme 4. Condensation reaction with terminal amine units. Reagents and conditions: (a) *tert*-butyl (2*S*,4*R*)-2-(aminomethyl)-4-fluoropyrrolidinecarboxylate, EDC·HCl, HOBt, Et_3N, CH_2Cl_2, for **15a–15c**, 79% for **15d**, for **15e**; (b) *tert*-butyl (2*S*,4*R*)-2-(aminomethyl)-4-fluoropyrrolidinecarboxylate, DMT-MM, DMF, 88% for **15f**, 85% for **15g**, 89% for **15h**, quant. for **15i**, 99% for **15j**; (c) TFA, CH_2Cl_2, 56% 2 steps for **6a**, 63% 2 steps for **6b**, 59% 2 steps for **6c**, 96% for **6d**, 79% 2 steps for **6e**, 45% for **6f**, 61% for **6g**, 84% for **6h**, 81% for **6i**, 45% for **6j**.

cyclopropylmethylamino moiety with cyclobutylamino moiety at position 6 on the imidazo[1,2-*b*]pyridazine group. Compound **6d** showed potent functional activity, favorable physical properties, good pharmacokinetics, and suitable plasma concentration level that led to excellent efficacy in collagen-induced arthritis models.

Acknowledgments

We are grateful to the members of Drug Metabolism & Pharmacokinetics Research Laboratories for their measurement and validation of physicochemical data.

We would like to express our sincere appreciation to Dr. T. Washio and Dr. N. Masubuchi for conducting the pharmacokinetic assays and their helpful discussions. We would also like to thank Dr. K. Suzuki and Ms. A. Kameda for their support in preparing the physicochemical data.

References and notes

1. Sen, R.; Baltimore, D. *Cell* **1986**, *47*, 921.
2. (a) Li, Q.; Verma, I. M. *Nat. Rev. Immunol.* **2002**, *2*, 725; (b) Hayden, M. S.; Ghosh, S. *Cell* **2008**, *132*, 344.
3. Brown, K. D.; Claudio, E.; Siebenlist, U. *Arthritis Res. Ther.* **2008**, *10*, 1.
4. Viatour, P.; Merville, M. P.; Bours, V.; Chariot, A. *Trends Biochem. Sci.* **2005**, *30*, 43.
5. Senftleben, U.; Karin, M. *Crit. Care Med.* **2002**, *30*, S18.
6. (a) Karin, M.; Lin, A. *Nat. Immunol.* **2002**, *3*, 221; (b) Coussens, L. M.; Werb, Z. *Nature* **2002**, *420*, 860; (c) Kim, H. J.; Hawke, N.; Baldwin, A. S. *Cell Death Differ.* **2006**, *13*, 738; (d) Perkins, N. D.; Gilmore, T. D. *Cell Death Differ.* **2006**, *13*, 759.
7. (a) Asagiri, M.; Takayanagi, H. *Bone* **2007**, *40*, 251; (b) Ruocco, M. G.; Maeda, S.; Park, J.-M.; Lawrence, T.; Hsu, L.-C.; Cao, Y.; Schett, G.; Wagner, E. F.; Karin, M. J. *Exp. Med.* **2005**, *201*, 1677.
8. Tak, P. P.; Firestein, G. S. J. *Clin. Invest.* **2001**, *107*, 7.
9. (a) Hayden, M. S.; Ghosh, S. *Genes Dev.* **2004**, *18*, 2195; (b) Häcker, H.; Karin, M. *Sci. STKE* **2006**, *357*, re13.
10. (a) DiDonato, J. A.; Hayakawa, M.; Rothwarf, D. M.; Zandi, E.; Karin, M. *Nature* **1997**, *388*, 548; (b) Mercurio, F.; Zhu, H.; Murray, B. W.; Shevchenko, A.; Bennett, B. L.; Li, J.; Young, D. B.; Barbosa, M.; Mann, M.; Manning, A.; Rao, A. *Science* **1997**, *278*, 860; (c) Woronicz, J. D.; Gao, X.; Cao, Z.; Rothe, M.; Goeddel, D. V. *Science* **1997**, *278*, 866.
11. Karin, M.; Yamamoto, Y.; Wang, Q. M. *Nat. Rev. Drug Discov.* **2004**, *3*, 17.
12. (a) Blake, S. M.; Swift, B. A. *Curr. Opin. Pharmacol.* **2004**, *4*, 276; (b) Burke, J. R.; Strnad, J. *Trends Pharmacol. Sci.* **2007**, *28*, 142.
13. The latest IKKβ inhibitors are reported in the following references and the previous references are cited in Ref. 15. (a) Dyckman, A. J.; Langevine, C. M.; Quesnelle, C.; Kempson, J.; Guo, J.; Gill, P.; Spergel, S. H.; Watterson, S. H.; Li, T.; Nirschl, D. S.; Gillooly, K. M.; Pattoli, M. A.; McIntyre, K. W.; Chen, L.; McKinnon, M.; Dodd, J. H.; Barrish, J. C.; Burke, J. R.; Pitts, W. J. *Bioorg. Med. Chem. Lett.* **2011**, *21*, 383; (b) Cushing, T. D.; Baichwal, V.; Berry, K.; Billedeau, R.; Bordunov, V.; Broka, C.; Cardozo, M.; Cheng, P.; Clark, D.; Dalrymple, S.; DeGraffenreid, M.; Gill, A.; Hao, X.; Hawley, R. C.; He, X.; Jaen, J. C.; Labadie, S. S.; Labelle, M.; Lehel, C.; Lu, P. P.; McIntosh, J.; Miao, S.; Parast, C.; Shin, Y.; Sjogren, E. B.; Smith, M. L.; Talamas, F. X.; Tonn, G.; Walker, K. M.; Walker, N. P.; Wesche, H.; Whitehead, C.; Wright, M.; Browner, M. F. *Bioorg. Med. Chem. Lett.* **2011**, *21*, 417; (c) Cushing, T. D.; Baichwal, V.; Berry, K.; Billedeau, R.; Bordunov, V.; Broka, C.; Browner, M. F.; Cardozo, M.; Cheng, P.; Clark, D.; Dalrymple, S.; DeGraffenreid, M.; Gill, A.; Hao, X.; Hawley, R. C.; He, X.; Labadie, S. S.; Labelle, M.; Lehel, C.; Lu, P. P.; McIntosh, J.; Miao, S.; Parast, C.; Shin, Y.; Sjogren, E. B.; Smith, M. L.; Talamas, F. X.; Tonn, G.; Walker, K. M.; Walker, N. P.; Wesche, H.; Whitehead, C.; Wright, M.; Jaen, J. C. *Bioorg. Med. Chem. Lett.* **2011**, *21*, 423; (d) Noha, S. M.; Atanasov, A. G.; Schuster, D.; Markt, P.; Fakhrudin, N.; Heiss, E. H.; Schrammel, O.; Rollinger, J. M.; Stuppner, H.; Dirsch, V. M.; Wolber, G. *Bioorg. Med. Chem. Lett.* **2011**, *21*, 577; (e) Xie, J.; Poda, G. I.; Hu, Y.; Chen, N. X.; Heier, R. F.; Wolfson, S. G.; Reding, M. T.; Lennon, P. J.; Kurumbail, R. G.; Selness, S. R.; Li, X.; Kishore, N. N.; Sommers, C. D.; Christine, L.; Bonar, S. L.; Venkatraman, N.; Mathialagan, S.; Brustkern, S. J.; Huang, H.-C. *Bioorg. Med. Chem.* **2011**, *19*, 1242; (f) Takahashi, H.; Shinoyama, M.; Komine, T.; Nagao, M.; Suzuki, S.; Tsuchida, H.; Katsuyama, K. *Bioorg. Med. Chem. Lett.* **2011**, *21*, 1758; (g) Avila, C. M.; Lopes, A. B.; Gonçalves, A. S.; da Silva, L. L.; Romeiro, N. C.; Miranda, A. L.; Sant'anna, C. M.; Barreiro, E. J.; Fraga, C. A. *Eur. J. Med. Chem.*

2011, *46*, 1245; (h) Miller, D. D.; Bamborough, P.; Christopher, J. A.; Baldwin, I. R.; Champigny, A. C.; Cutler, G. J.; Kerns, J. K.; Longstaff, T.; Mellor, G. W.; Morey, J. V.; Morse, M. A.; Nie, H.; Rumsey, W. L.; Taggart, J. T. *Bioorg. Med. Chem. Lett.* **2011**, *21*, 2255; (i) Kim, S.; Jung, J.-K.; Lee, H.-S.; Kim, Y.; Kim, J.; Choi, K.; Baek, D.-J.; Moon, B.; Oh, K.-S.; Lee, B.-H.; Shin, K.-J.; Pae, A.-N.; Nam, G.; Roh, E.-J.; Cho, Y.-S.; Choo, H. *Bioorg. Med. Chem. Lett.* **2011**, *21*, 3002.

14. Shimizu, H.; Tanaka, S.; Toki, T.; Yasumatsu, I.; Akimoto, T.; Morishita, K.; Yamasaki, T.; Yasukochi, T.; Iimura, S. *Bioorg. Med. Chem. Lett.* **2010**, *20*, 5113.
15. Shimizu, H.; Yasumatsu, I.; Hamada, T.; Yoneda, Y.; Yamasaki, T.; Tanaka, S.; Toki, T.; Yokoyama, M.; Morishita, K.; Iimura, S. *Bioorg. Med. Chem. Lett.* **2011**, *21*, 904.
16. Lipinski, C. A.; Lombardo, F.; Dominy, B. W.; Feeney, P. J. *Adv. Drug Deliv. Rev.* **2001**, *46*(1–3), 3.
17. Madin–Darby canine kidney cell permeability.
The cell permeability of the selected compounds was determined with Madin–Darby canine kidney (MDCK) cells. MDCK cells were maintained in Minimum Essential Medium containing 10% (v/v) fetal bovine serum, a penicillin–streptomycin mixture and L-glutamine. For the transport assay, cells were seeded into HTS 24-well transwells at 1.65×10^5 cells/ml, and grown for 6 days after seeding to allow the formation of a cell monolayer. Transport buffer was prepared using $NaHCO_3$ (final 0.35 g/l), D-glucose (final 3.5 g/l), Hepes (final 10 mM), $CaCl_2$ (final 0.14 g/l) and $MgSO_4$ (final 0.098 g/l) in 10× Hanks' Balanced Salt Solution, and then adjusted to pH 6.0 or 7.4 with 1 M HCl or 1 M NaOH. For each test compound, a 100 μl of dosing solution containing one of the compounds at a concentration of 10 μM in transport buffer (pH 6.0) was added to the apical (A) side of the monolayer. A 600 μl of blank solution containing 4% (w/v) BSA in transport buffer (pH 7.4), which was re-adjusted to pH 7.4, was added to the basolateral (B) side of the monolayer. Metoprolol was used as a positive control. After 1 h of incubation at 37 °C, aliquots of the basal solutions were analyzed on an LC/MS/MS system. For each compound, Eq. 1 was used to calculate the apparent permeability coefficient (P_{app}) from the LC/MS/MS-determined concentration in the basolateral compartment (C_b, μM) and the initial 10 μM concentration in the donor compartment. In the following equation, 3600 s is the total time for the measurement of compound flux, and 0.33 cm^2 is the area of the transwell filter.

$$P_{app}(10^{-6}\ \mathrm{cm/s}) = (C_b \times 600\ \mu\mathrm{l})/(10\ \mu\mathrm{M} \times 3600\ \mathrm{s} \times 0.33\ \mathrm{cm}^2) \quad (1)$$

18. Howard, J. A. K.; Hoy, V. J.; O'Hagan, D.; Smith, G. T. *Tetrahedron* **1996**, *52*, 12613.
19. Stability assay in mouse/rat liver microsome.
Test compound (final 1 μM) was incubated with male CD1 mouse liver microsome/male IGS-SD rat liver microsome (final 0.1 mg/ml, $n = 2$) in sodium phosphate buffer (pH 7.4) for 20 min at 37 °C. Assays were started by the addition of NADPH at 37 °C and stopped by the addition of acetonitrile after incubation for 30 min. The sample was ice-stored more than 30 min, followed by centrifuged at 3500 rpm for 10 min at 4 °C. The supernatant was applied for the analysis of supernatant by LC/MS/MS system. The remaining % of test compound was calculated determined by the following equation:
Microsomal stability (% remaining) = {(Peak Area Ratio of test compound at 30 min)/(Peak Area Ratio of test compound at 0 min)} × 100
20. Distribution coefficient.
Equal amounts of pH 7.4 phosphate buffered saline (PBS) and 1-octanol were shaken and left for over 12 h. The upper layer (1-octanol) and lower layer (PBS) were collected individually. Each compound was dissolved in 1-octanol or PBS (200 μM). The same amount of either PBS or 1-octanol was added and the mixture was shaken vigorously for 30 min at room temperature. Then, both phases were separated and assayed by HPLC or LC/MS. Log $D_{7.4}$ was calculated by the following equation: Log $D_{7.4}$ = log(Peak area of compound in 1-octanol/Peak area of compound in PBS)
21. Membrane permeability assay.
The membrane permeability coefficients were assayed using PAMPA Evolution™. The filter membrane of a donor plate was coated with phospholipids (GTI-0 lipid solution). At concentrations of 50 μM (containing of 5% DMSO, pH 7.4), all the compounds were placed in a donor plate. The acceptor plate was filled with Acceptor solution (ASB-7.4). The acceptor plate was then stacked over the donor plate for 4 h incubation at 25 °C. The compound concentrations were assayed for both plates with a UV spectrometer. The effective permeability ($P_{e7.4}$) was calculated with PAMPA Evolution Command Software.
22. Compound **6d** showed more than 50% inhibition against 6 kinases at 0.2 μM out of 250 kinases.
23. Protein binding studies.
To the 495 μl of serum samples of male BALB/c mice or female Wister–Lewis rats, 5 μl of test compound (10 μg/ml, 20% acetonitrile aqueous solution) was added and stirred weakly (final 100 ng/ml, $n = 2$). The mixture was shaken for 4 h at 37 °C in Rapid Equilibrium Dialysis Device.
To the 50 μl of the mixture, 50 μl of buffer was added. The blank serum was prepared in the same manner.
After addition of the 120 μl of internal standard acetonitrile solution to the samples, respectively and mixed, followed by centrifugation at 1800×*g* for 5 min at 4 °C. The supernatants were filtered (0.45 μm) and the concentrations of the test compounds were determined by an LC/MS/MS method.
24. Pharmacokinetic studies on mice.
Female BALB/c mice (7 weeks of age, $n = 3$) were used. The fed mice were orally administered the test compound at a dose of 30 mg/kg/10 ml suspended in 0.5% (w/v) methyl cellulose aqueous solution. Blood samples were collected at 0.5, 1, 2, 4, 8 and 24 h after administration. Blood samples (0.5 ml) were ice-stored, followed by centrifugation at 1800×*g* for 5 min at 4 °C. The plasma fractions were subsequently stored in a −20 °C freezer until being analyzed. The concentrations of the test compounds were determined by an LC/MS/MS method. The plasma concentrations versus the time data were analyzed by non-compartment approaches.
25. Pharmacokinetic studies on rats.
Female Wistar–Lewis rats (7–8 weeks of age, $n = 3$) were used. The fed rats were orally administered the test compound at doses of 30 mg/kg/2 ml suspended in 0.5% (w/v) methyl cellulose aqueous solution. Blood samples (0.3 ml) were collected at 0.5, 1, 2, 4, 8 and 24 h after administration. These analytical samples were stored at room temperature, followed by centrifugation at 1800×*g* for 5 min at 4 °C. The plasma fractions were subsequently stored in a −20 °C freezer until being analyzed. The concentrations of the test compounds were determined by an LC/MS/MS method. The plasma concentrations versus the time data were analyzed by non-compartment approaches.
26. Induction and assessment of collagen-induced arthritis in mice.
Female DBA/1 mice (7 weeks of age, $n = 7$) were immunized by an intradermal injection at the base of the tail with 0.1 ml of emulsion containing 1.5 mg/ml of bovine type II collagen in Freund's complete adjuvant. Twenty-one days later, mice were boosted by an intradermal injection at the abdomen with a total of 0.1 ml of same emulsion. Mice were treated with or without a test compound from the day of the second injection. Clinical severity of inflammation was scored periodically on a scale of 0–3 based on criteria as follows: 0, normal; 0.5, swelling of one digit; 1, swelling of more than two digits or redness of paw; 2, swelling of partial paw; 3, swelling of entire paw.
27. Induction and assessment of collagen-induced arthritis in rats.
Female Dark Agouti rats (9–10 weeks of age, $n = 6$) were immunized by an intradermal injection at the back with a total of 0.2 ml of emulsion containing 250 μg/ml of bovine type II collagen in Freund's incomplete adjuvant. Seven days later, rats were boosted by an intradermal injection at the base of the tail with a total of 0.1 ml of the same emulsion. Rats were treated with or without a test compound from the day of the second injection. Hind paw volume was measured periodically from induction of arthritis using a water displacement plethysmometer. Paw swelling was expressed as the mean of the both hind paw volumes of the change from the day before the boost.
28. Inhibition assay of LPS-induced TNFα production by rat whole blood cell.
Whole blood was collected from Lewis rat in heparinized tubes, and plated in a 96-well plate at 2×10^5 cells/well suspended in RPMI-1640 containing 10% fetal bovine serum, 25 mM HEPES, 50 U/ml penicillin and 50 μg/ml streptomycin. Cells were pretreated with various concentrations of test compounds just before stimulation with 1 μg/ml LPS. After 4 h of incubation at 37 °C in 5% CO_2, the culture supernatants were harvested by centrifugation (2000 rpm at 5 min, 4 °C). TNFα concentration in the supernatants was measured using ELISA kit according to the manufacturer's instructions.
29. (a) Imanishi, M.; Tomishima, Y.; Itou, S.; Hamashima, H.; Nakajima, Y.; Washizuka, K.; Sakurai, M.; Matsui, S.; Imamura, E.; Ueshima, K.; Yamamoto, T.; Yamamoto, N.; Ishikawa, H.; Nakano, K.; Unami, N.; Hamada, K.; Matsumura, Y.; Takamura, F.; Hattori, K. J. *Med. Chem.* **2008**, *51*, 1925; (b) Ranbaxy Laboratories Limited, WO2009156966, **2009.**; (c) Ishiyama, T.; Takagi, J.; Yonekawa, Y.; Hartwig, J. F.; Miyaura, N. *Adv. Synth. Catal.* **2003**, *345*, 1103.